Acta Materialia 284 (2025) 120529

Contents lists available at ScienceDirect

Acta Materialia

journal homepage: www.elsevier.com/locate/actamat

Full length article

Advancing the thermodynamic modeling of multicomponent phases in hydrogen-para-equilibrium

Peter Hannappel [a,b,*], Felix Heubner [a,*], Mateusz Balcerzak [a,c], Thomas Weißgärber [a,b]

[a] Fraunhofer Institute for Manufacturing Technology and Advanced Materials IFAM, Dresden Branch, Dresden, Germany
[b] TUD Dresden University of Technology, Faculty Mechanical Engineering, Institute of Materials Science, Chair Powder Metallurgy, Dresden, Germany
[c] Institute of Materials Science and Engineering, Poznan University of Technology, Poznań 61-138, Poland

ARTICLE INFO

Keywords:
Calphad thermodynamics
La–Ce–Ni–H
Metal hydrides
Python
Database

ABSTRACT

We present an advanced approach for the thermodynamic modeling of metal hydrides within the Calculation of Phase Diagrams (CALPHAD) framework. As the traditional CALPHAD method requires significant and time-consuming manual input, often introducing biases into the assessment process, we present a novel solution to automate this. The core of our approach is the development of an open-source, Python-based computational tool designed to calculate para-equilibrium states in hydrogen-multicomponent phases. This tool facilitates a semi-automatic pathway to enhance the CALPHAD evaluation procedure, significantly reducing manual input. We validated our approach by rapidly assessing the (Ce,La)Ni_5–H system, a representative material system with significant implications for metal hydride-based hydrogen applications. Our method confirms existing data and reveals new insights into this system's sorption properties and phase behavior. Using our Python-based tool to optimize parameter sets and calculate Pressure-Composition-Isotherms (PCI), we demonstrate the feasibility of predicting temperature-dependent plateau pressures and hydrogen capacities of multicomponent metal hydrides. This work holds significant potential for future applications in designing hydrogen storage materials, predicting their properties, and extending the methodology to other metal hydride systems.

1. Introduction

The importance of metal hydrides in the hydrogen economy covers a wide range of applications, including energy storage, hydrogen compression, purification and metal hydride-based cooling systems [1–3]. In each application scenario, the sorption properties for relevant temperature conditions, such as absorption/desorption pressures, hydrogen capacities, and reaction enthalpies, must be precisely tuned and optimized.

Recently, many efforts have been made to model the sorption properties to overcome the intuition-based try-and-error approach when designing new alloy compositions. While machine-learning tools provide a quick compilation of big data over a vast amount of structures and elements, the models lack precise predictions of the sorption properties [4–6]. In contrast, CALculation of PHase Diagrams (CALPHAD) is a well-established method for accurate thermodynamic modeling of multicomponent phases. Despite its widespread use, the traditional evaluation procedures within CALPHAD require significant manual input from evaluators, including selecting appropriate sublattice models, parameter sets, weights, and initial guesses, particularly for gradient-based optimizers [7].

Thermodynamic principles significantly influence the determination of ideal sorption properties in metal hydrides. This is demonstrated by the ability to derive these properties from phase diagrams, so-called Pressure-Composition-Isotherms (PCI), which describe the hydrogen content as a function of the hydrogen pressure at constant temperature. While binary metal-hydrogen systems have long been modeled using the Compound Energy Formalism (CEF) [8] within the CALPHAD method [9], more complex systems have only recently been investigated [10–13]. Whereas most of these higher-order systems are pseudo-binary systems [10,11,13], Pinatel et al. found a workaround to assess the La(Al,Ni)$_5$–H system in ortho-equilibrium [12]. In addition to these time-intensive assessments, thermodynamic modeling approaches outside the CALPHAD method have been applied lately to model and predict sorption properties over various chemical elements within the para-equilibrium state [14]. However, these methods lack the incorporation of experimental data.

Modeling metal hydrides within the CEF presents a distinct challenge due to the para-equilibrium states arising from the high hydrogen gas diffusion rate at low temperatures. This allows the hydrogen concentration to change while the metal structure remains static [15].

* Corresponding authors.
E-mail addresses: peter.hannappel@ifam-dd.fraunhofer.de (P. Hannappel), felix.heubner@ifam-dd.fraunhofer.de (F. Heubner).

https://doi.org/10.1016/j.actamat.2024.120529
Received 29 July 2024; Received in revised form 11 October 2024; Accepted 31 October 2024
Available online 12 November 2024

The aspect of para-equilibrium, particularly when modeling multicomponent phases (defined here as phases with more than one element occupying a single sublattice), complicates the consistency of metal elements across both sides of the solid-hydrogen reaction in the region of the pressure plateau.

Addressing these gaps, this paper introduces:

1. An open-source Python-based code for calculating para-equilibria for hydrogen — multicomponent phases within the CEF.
2. A semi-automatic pathway to enhance the assessment process within the CALPHAD framework, reducing manual user input and enabling the evaluation of systems with many components.
3. The validation of the proposed approach through the rapid assessment of the (Ce,La)Ni_5–H system.

Finally, this work presents the first reported thermodynamic evaluation procedure of multicomponent metal hydrides in the para-equilibrium state within the CALPHAD framework. This procedure allows accurate calculations of hydrogen sorption properties while incorporating experimental data. It paves the way for constructing a comprehensive thermodynamic database for metal hydrides, enabling faster design routes for hydrogen applications.

2. Thermodynamic modeling

2.1. Open-source program to calculate para-equilibrium states

To create a new assessment procedure (Section 2.2), a Python program was developed to calculate the para-equilibrium state of a thermodynamic data set. The Python files can be accessed at https://github.com/PHannapp/para-equilibrium-thermodynamic-modeling with a tutorial in the Supplementary Material (Section S1-2) and are briefly described as follows.

The user defines the sublattice model within the CEF in the thermodynamic database (*database.py*). The database contains Gibbs energy terms for the solid and gas phases, with either parameters or optimization variables. These terms are defined as functions in Python notation, with the function names representing the phase structure and returning (optionally temperature or pressure dependent) terms and optimization variables.

The function names representing the reference energy of the end-members are denoted with a *G*, followed by the elements on the sublattices. Each sublattice is separated with an underscore. Solid-state elements consist of two letters, whereas in interstitial sublattices, hydrogen and vacancies are denoted with *H* and *V*, respectively. Variables within the functions are optimized and declared with the prefix *V*, followed by incrementing integers starting with *V0*.

Interaction terms are denoted with *L*, followed by the elements on the sublattices. Again, each sublattice is separated by an underscore. For the mixing site, both elements in alphabetical order must be declared. Mixing on the interstitial sites is indicated with *HV* (Hydrogen-Vacancy). The interaction order from 0 to 2 is denoted at the end.

Equations.py calculates the internal equilibrium for the solid phase. After defining the multiplicity of each site, the program minimizes the solid's Gibbs energy by calculating the trajectory of the interstitial site occupation with a global optimizer (differential evolution [16]) using the definitions in the thermodynamic database.

The script *Calculate_PCI.py* searches for the miscibility gap in the solid phase by identifying inflection points in the Gibbs energy curve and creating a common tangent around them. After identifying all miscibility gaps, a hydrogen concentration can be assigned to the solid phase at each pressure point by creating common tangents with the gas phase.

In summary, the available code is capable of the following:

1. Calculate the Gibbs energy for a fixed composition with the Redlich–Kister polynomial.
2. Determine the minimized Gibbs energy curve for the hydrogen occupation trajectory of the metal hydride.
3. Calculate the partially minimized energy of the hydrogen (gas) – metal (hydride) – system. This allows for the calculation of the experimentally observed PCI diagrams under para-equilibrium.

In the next chapter the concept of an advanced assessment procedure, implementable within *Python* is proposed.

2.2. Proposing a new assessment procedure

Fig. 1 shows a scheme of the semi-automatic assessment procedure. The user provides manual input to define the sublattice model and optimize variables in the database file. This work includes the entropic and enthalpic terms for the reference energies and the temperature-independent interaction terms up to the first order for the non-ideal mixing energy in the deduced parameter space. The number of possible parameter sets N that are automatically optimized amounts to:

$$N = 2^n. \tag{1}$$

Here, n is the number of optimization variables in the thermodynamic database. To control the size of the parameter space, each (pseudo-) binary and ternary system is optimized separately. Ternary systems are optimized after and based on the optimization of the binary systems. When no experimental data is available for the binary system but for the ternary, both are optimized simultaneously, at the expense of computational time.

Boundaries on the optimization variables are mandatory since the variables are optimized with a global minimization algorithm. Suitable boundaries can be defined using ab initio calculations. The parameter sets are optimized by minimizing the root mean square deviation (RMSD) based on the experimental and calculated plateau pressures, phase boundaries, and pressure-hydrogen concentration pairs in the solution phases (alpha-, beta- or gamma-phase). Optional weightings of the different experimental points can be included in the RMSD function. This work used the differential evolution algorithm from Python's SciPy library to minimize the RMSD function [16]. The time for the optimization procedure, t_{opt}, is calculated as:

$$t_{opt} = iter * popsize * n_{\neq} * t_{cal}, \tag{2}$$

where $iter$ represents the number of iteration steps, $popsize$ refers to the population size, t_{cal} is the time required to calculate one RMSD function, and $n_{\neq}$ represents the number of optimization variables with unequal upper and lower boundaries.

The initial value of a given parameter set is determined by the optimized value of the next lower-order parameter set. If no lower-order parameter sets are available, the initial values can be determined through brute force to obtain a parameter set that returns an RMSD below a previously defined threshold.

To achieve a balance between a minimal amount of thermodynamic parameters and optimized fitting values, a penalty factor is added to the RMSD of the global optimizer for each parameter that is not equal to zero:

$$pRMSD = RMSD + p * n_{\neq 0}, \tag{3}$$

where p is the penalty factor, tunable by the user. p should be fitted to the RMSD function. In this work, a penalty factor of 2 was found to yield reasonable results.

2.3. Literature review of the (Ce,La)Ni_5–H system

2.3.1. Structure

Recent AB_5–H system thermodynamic evaluations used the one-sublattice model for the hydrogen-vacancy interstitial sites with seven interstitial sites per formula unit [12]. This model is a reasonable choice based on the calculated $P6_3mc$ crystal structure [17]. However, recent

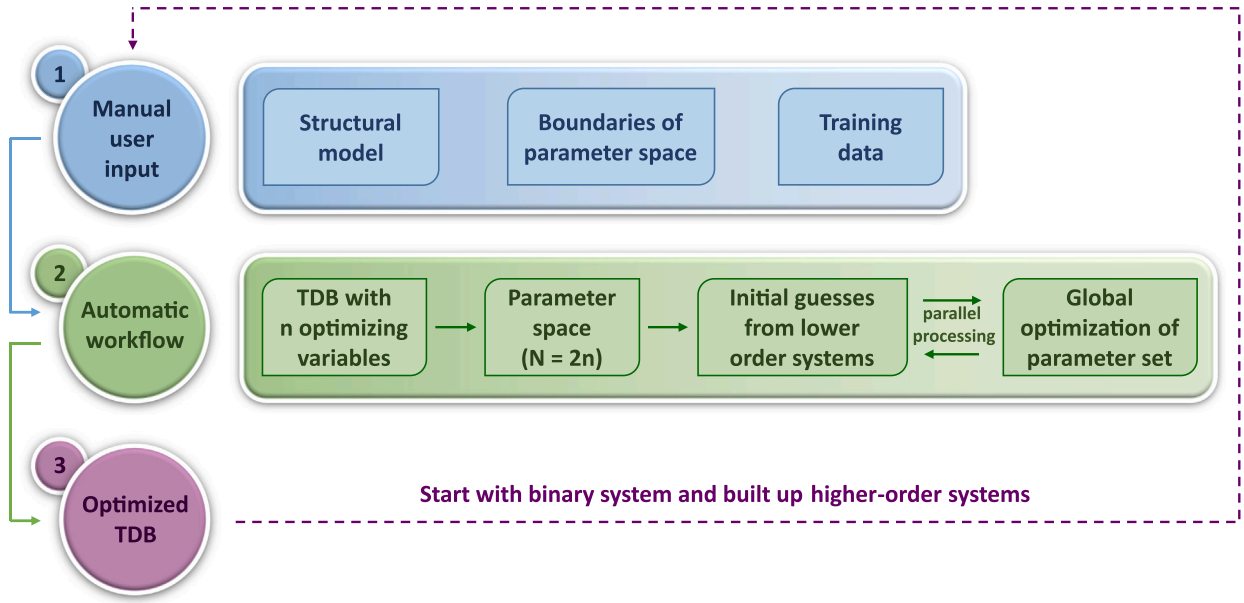

Fig. 1. Scheme of the proposed semi-automatic assessment workflow within the CALPHAD framework. In comparison to traditional assessment procedures, the optimal set of parameters is evaluated from all possible combinations within the parameter space (containing n optimization variables of the thermodynamic database - TDB), omitting the need to specify initial guesses.

results have shown that this sublattice model can represent plateau pressures but cannot sufficiently model plateau boundaries, as apparent in experimental studies [12].

Furthermore, in the $P6_3mc$ structure, the metal atoms occupy the 2a and 2b sites. Herbst et al. calculated the formation energies of different hydrogen site occupations within the $LaNi_5$–H system [18]. They found that the preferred hydrogen occupation is the ($2b6c_16c_2$) configuration, while the $LaNi_5H_1$, $LaNi_5H_6$, and $LaNi_5H_7$ are stable compounds on the convex hull.

Therefore, we tested the new sublattice model $(Ce,La)(Ni)_5(H,Va)_1(H,Va)_6$, where the interstitial sublattices with multiplicity one and six, correspond to the 2b site and ($6c_16c_2$) sites, respectively. The merging of these two distinct 6c sites was done to reach a compromise between physical accuracy and model complexity. The addition of a third hydrogen-vacancy sublattice alone would double the number of end members, not to mention the interaction parameters.

2.3.2. *Pressure-composition-isotherm data*

Three distinct assessments may be conducted for each PCI experiment: absorption, desorption, and equilibrium. The equilibrium is assumed to lie between absorption and desorption [19]. To ascertain the equilibrium in this study, the logarithmic average between the absorption and desorption isotherm is calculated.

The thermodynamic data for the $LaNi_5$–H system (from PCI data) has been extensively analyzed elsewhere [20,21]. Experimental data for the $CeNi_5$–H system is limited. We collected PCI data from three publications [20,22,23]. The plateau pressures are consistent, but the hydrogen content at the plateau boundaries varies between the publications. The discrepancies of the hydrogen capacities could be due to slow sorption kinetics, mainly if the alloys were not fully activated [23]. In summary, the hydrogen mole fraction x_H at the beginning of the plateau is estimated to be around $x_H = 0.05 - 0.1$, while at the end of the plateau, it is around $x_H = 0.4 - 0.5$.

Regarding the $Ce_xLa_{1-x}Ni_5$–H system, the literature data is overall consistent for $x < 0.5$. However, for $x > 0.5$, the hydrogen fractions at the plateau boundaries vary significantly. Klyamkin et al. [23] and Zhou et al. [24] report a high solubility of hydrogen in the hydride for the $Ce_{0.8}La_{0.2}Ni_5$ compound ($x_H = 0.45 - 0.48$), while Odysseos et al. [25] indicate a strong decrease in the hydrogen capacity for cerium-rich compounds. The absorption experiment revealed that the $Ce_{0.8}La_{0.2}Ni_5$ compound had a hydrogen capacity of only $x_H = 0.4$.

To validate the trajectory of the hydrogen capacity on the cerium-rich side, we conducted additional measurements on the $Ce_xLa_{1-x}Ni_5$ system (up to $x = 0.65$).

3. Materials and methods

The following synthesis and characterization procedures were conducted to determine the proper experimental data for evaluating the $(Ce,La)Ni_5$–H system.

The samples $Ce_{0.2}La_{0.8}Ni_5$, $Ce_{0.4}La_{0.6}Ni_5$, and $Ce_{0.65}La_{0.35}Ni_5$ were produced from high-purity elemental metals: Ce (99.9%, Osnabruegge GmbH), La (99.9%, VWR International GmbH) and Ni (99.95%, Thermo Fisher GmbH). Metal pieces in mm to cm size were used.

The arc-melting method was employed under an argon atmosphere with an actively cooled Cu crucible. The metals were melted three times per side for two minutes and flipped in between. The single-phase crystal structure and homogeneous chemical composition of $Ce_{0.65}La_{0.35}Ni_5$ was proved with an optical microscope, SEM and EDX, Carrier Gas Hot Extraction, and X-ray diffraction analysis (Supplementary Information, Section S4). The crystal structure of the other samples was proven to be a single *P6/mmm* phase (Supplementary Information, Fig. S6).

XRD analysis was conducted (Empyrean, Malvern Panalytical GmbH, Co-$K_{\alpha 1}$-radiation ($\lambda = 1.789\,010$ Å), 2θ: 6-148 °, step size: 0.0084 °, time per step: 600 s) and analyzed using the Rietveld method with HighScore (Malvern Panalytical GmbH) and TOPAS [26].

Hydrogen sorption tests were conducted to detect weight differences during sorption. The experiments were performed up to 130 bar at 283, 298 and 313 K using a magnetic suspension balance (Waters GmbH). These experiments are used to calculate the reaction enthalpy through the application of the van't Hoff equation. The samples were stored and prepared in an inert argon atmosphere. The transport was done in air as a bulk piece of around 2 g. The samples were activated by cycles of high hydrogen pressure (above plateau) and vacuum at 293 K until no difference in the measured capacities could be observed. Between each cycle, the vacuum (10^{-3} Pa) was maintained for at least 30 min. The threshold to define equilibrium was defined as a mass change rate of 10 µg/min over a period of 10 min. This equals a relative mass change of 5×10^{-3} wt.-% per minute.

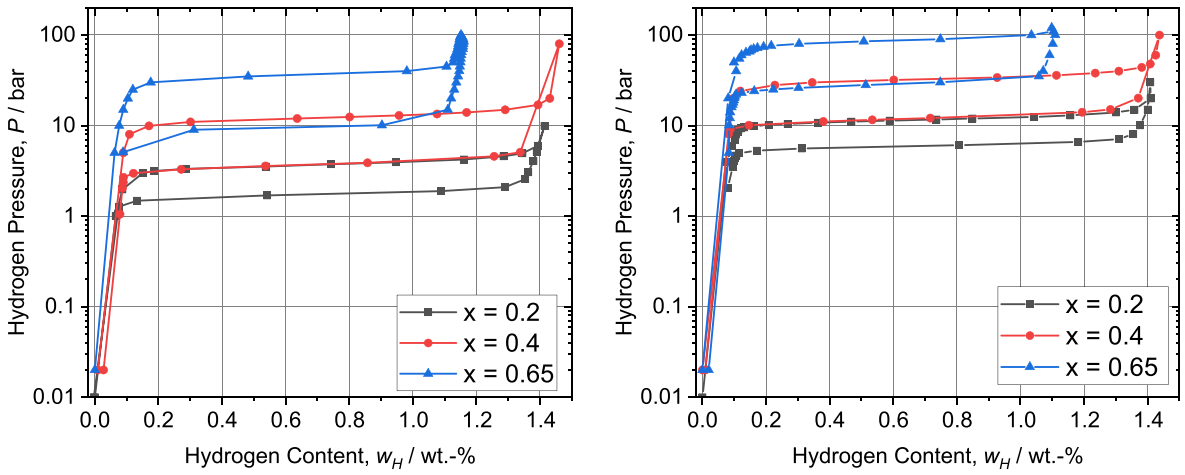

Fig. 2. Pressure-composition isotherms of $Ce_xLa_{1-x}Ni_5$–H at 283 K (left) and 313 K (right). The upper curves present the hydrogen absorption, while the lower ones show hydrogen desorption.

4. Results and discussion

4.1. Sorption experiments

Fig. 2 and Fig. S8 present the experimental results of the sorption experiments of our $Ce_xLa_{1-x}Ni_5$ alloys. This data allowed us to validate the findings from other publications:

- A (nearly) constant solubility of the alpha-phase can be seen, independent of the alloy chemical composition and the temperature.
- The plateau end (beta-phase composition at plateau pressure) strongly diminishes for x > 0.4. This is in accordance with the results from Odysseos et al. who found a threshold of $Ce_{0.5}La_{0.5}Ni_5$ [25] but in contrast to the experiments of Zhou et al. and Klyamkin et al. [23,24]. To ensure that no kinetic limitations falsify our data, we conducted the same measurement with a lower equilibrium threshold of a mass change rate of 4 µg/min over a period of 10 min. No changes in the PCI data could be detected, thereby proving the absence of kinetic limitations in the experiments.
- The slight increase in hydrogen capacity for (x = 0 − 0.5) was reproduced [24,25].
- The reaction enthalpies are consistent with those reported by Zhou et al. [24], as can be seen in Fig. 4. (We summarized the numerical values in Table S4 of the SI.) In contrast, the enthalpy data reported by Odysseos et al. [25] are contradictory, with the absorption experiments yielding very high values. However, the plateau pressures in their studies correlate with the findings in this work, suggesting that the discrepancies may be due to calculation errors.

4.2. Modeling approach

The (Ce,La)Ni_5–H system was assessed with the proposed workflow (Fig. 1). Firstly, the ternary $LaNi_5$–H and $CeNi_5$–H systems were optimized using 11 optimization variables (three formation enthalpy terms and eight interaction terms of zeroth and first order) each. As the formation enthalpies are always included as optimization variables, the parameter space consists of 256 parameter sets for each system. The formation entropies were determined as the sum of the entropic term of the alloy and the entropy of the gas phase ($130\,J\,mol^{-1}\,K^{-1}$ per H_2, [9]). More complex formulations for the Gibbs energy of the endmembers were disregarded, as the model complexity must scale with the complexity of the experimental input parameters. The thermodynamic data of the metallic endmembers ($LaNi_5$, $CeNi_5$) were taken from previous assessments [10,27]. Secondly, the quaternary system was optimized with eight optimization variables (256 parameter sets) consisting of zeroth and first order interaction terms. The total computational time for optimizing the ternary and quaternary systems was 2296 core-hours. The optimized parameter sets are saved in the MongoDB file in the Supplementary Materials section.

Table 1
Optimized parameter set for the (La,Ce)Ni_5–H system. The notation of the parameters is explained in Section 2.1.

Parameter	Value	Reference
Endmembers		
GLA_NI_V_V	$-154674 + 30.6215 * T$	[10]
GLA_NI_H_V	$-153101 + (30.6215 + 61) * T$	This work
GLA_NI_V_H	$-216752 + (30.6215 + 366) * T$	This work
GLA_NI_H_H	$-268858 + (30.6215 + 427) * T$	This work
GCE_NI_V_V	$-197460 + 24.3084 * T$	[27]
GCE_NI_H_V	$-128606 + (24.3084 + 61) * T$	This work
GCE_NI_V_H	$-230655 + (24.3084 + 366) * T$	This work
GCE_NI_H_H	$-258147 + (24.3084 + 427) * T$	This work
Interaction terms for ternary systems		
LLA_NI_H_HV_1	−22942.8	This work
LCE_NI_V_HV_1	3565.8	This work
LCE_NI_H_HV_0	−141446	This work
LCE_NI_HV_H_0	−22772.3	This work
Interaction terms for quaternary systems		
GCELA_NI_H_V_0	74202	This work
GCELA_NI_H_V_1	−61141	This work
GCELA_NI_H_H_0	−38562	This work

4.3. Modeling results

The optimized parameter set is displayed in Table 1. Fig. 3 shows the occupation of site fractions for the ternary systems at 273 K, along with normalized enthalpy differences to the metallic compound and one H_2 molecule. The thermodynamic model indicates that hydrogen initially occupies the 6c-sites, reaching a site fraction of approximately $y_{6c} = 0.2$. This is followed by the complete filling of the 2b-sites. Subsequently, the 6c-sites are further occupied. The primary distinction between the hydrogenation of $LaNi_5$ and $CeNi_5$ is the hydrogen content when the 2b-sites begin to fill up.

Interestingly, the formation enthalpy of the $LaNi_5H_7$ compound is approximately the same as that of the $CeNi_5H_7$ phase. For both systems, only the terminal phases are on the convex hull. The significant difference lies in the formation enthalpy of the ANi_5H_1 endmember,

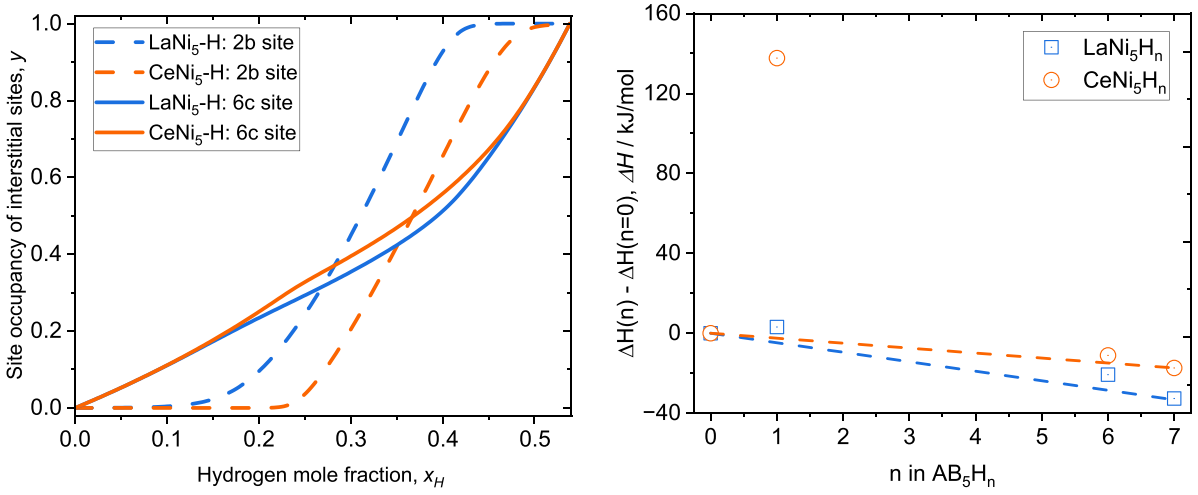

Fig. 3. The occupation of the hydrogen-vacancy sites of the ternary compounds (left) and the convex hull of the endmembers of the optimized values (right) in Table 1. (For interpretation of the references to color in this figure legend, the reader is referred to the web version of this article.)

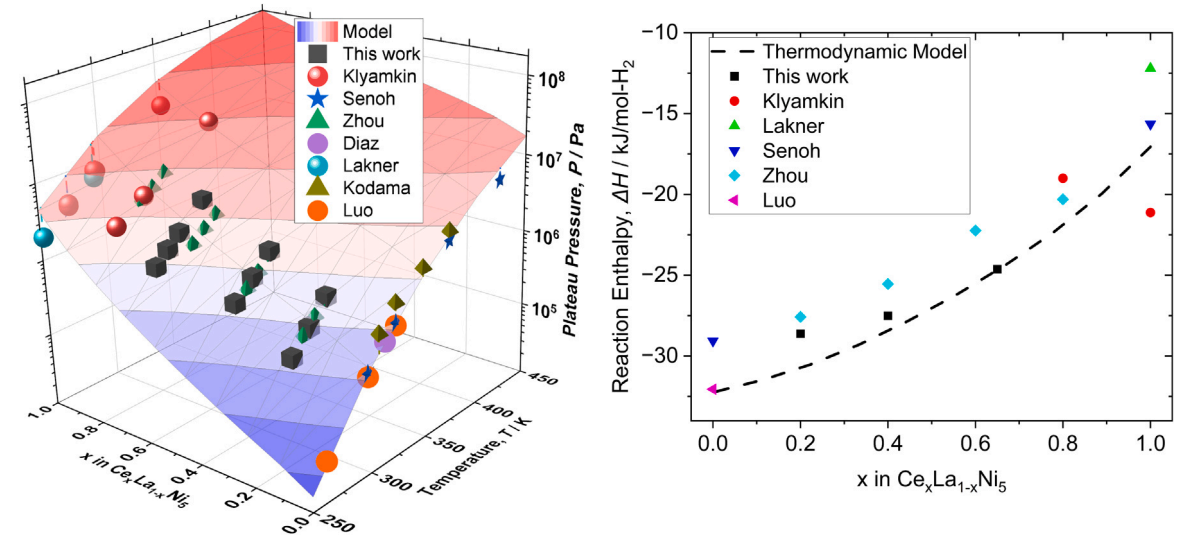

Fig. 4. Comparison of the plateau pressures, calculated with the thermodynamic model with PCI data from this work and literature [20–24,28,29] in 3D (left) and converted to the reaction enthalpy (right). (For interpretation of the references to color in this figure legend, the reader is referred to the web version of this article.)

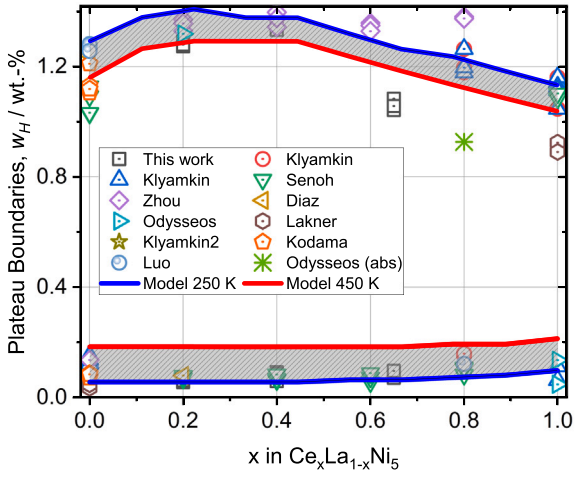

Fig. 5. Comparison of the thermodynamic model with the plateau boundaries from PCI data from this work and literature [20–25,28,29]. The thermodynamic model is calculated for a temperature range from 250 (blue) to 450 K (red).

which is much more unstable in the $CeNi_5$–H system. This difference leads to a later occupation of the 2b sites in the $CeNi_5$–H system than in the $LaNi_5$–H system.

Notably, the thermodynamics of the ternary systems can be best described by the interaction in the 6c sublattices. In the $CeNi_5$–H system, there is a very strong negative interaction. This favors a mixing of hydrogen and vacancies and, therefore, makes a complete occupation of the 6c site with hydrogen energetically unfavorable and results in lower capacities. In contrast, the $LaNi_5$–H system requires only one interaction term, around 1/6 of the corresponding interaction term in the $CeNi_5$–H system. Therefore, a full occupation is more favorable in $LaNi_5$–H, as represented in the high hydrogen solubilities in this system. We want to emphasize, that the reduction in the complexity of the sublattice model influences the physical interpretation of the site fillings. By merging the two distinct Wyckoff sites $6c_1$ and $6c_2$, distinct hydrogen occupation behaviors are averaged, potentially obscuring specific site preferences and energy differences.

Fig. 4 and Fig. S9–S15 illustrate the extracted plateau pressures from experimental PCI data plotted against the model results for the quaternary system. The reaction enthalpies are calculated from the plateau pressures, by fitting them to the Van't Hoff equation with

linear regression. Within the CALPAHD model, plateau pressures within the temperature range from 250 to 450 K were included. The results confirm earlier assessments by Pinatel et al. [12] that different publications provide complementary pressure data and that the plateau pressures can be accurately modeled using the CALPHAD method. The only discrepancy is in the $CeNi_5$ phase, where the experimental data varies significantly. This discrepancy is also evident when examining the reaction enthalpies. The experiments of Klyamkin et al. [23] show twice the reaction enthalpy compared to the experiments of Lakner et al. [22]. This difference could be due to the high pressures required for the hydrogenation of $CeNi_5$. In addition to the systematic errors that can be introduced by the measurement procedure when using Sieverts-type apparatus, the sole application of the ideal gas law can also introduce significant errors.

In Fig. 5, the plateau boundaries (alpha- and beta-phase solubility at plateau pressure) are compared with the model results. Among the ternary compounds, $LaNi_5H_x$ exhibits a much higher capacity than $CeNi_5H_x$. At 250 K and 450 K, $LaNi_5$ can be hydrogenated up to $LaNi_5H_{5.6}$ and $LaNi_5H_5$, respectively. On the other hand, $CeNi_5$ exhibits reduced hydrogen capacities, ranging from $CeNi_5H_{4.5–4.7}$ in the same temperature range.

The highest hydrogen solubility shows the $Ce_{0.22}La_{0.78}Ni_5$ alloy with a concentration of up to 6.14 hydrogen atoms per formula unit.

The solubility of the alpha-phase remains relatively constant. At 300 K the range of hydrogen contents varies from $Ce_xLa_{1-x}Ni_5H_{0.35}$ to $Ce_xLa_{1-x}Ni_5H_{0.58}$. The two interstitial sublattice model provide a significant advantage in modeling the alpha-phase's relatively low and constant solubilities while representing varying beta-phase contents simultaneously.

5. Conclusions

An open-source code is presented for calculating phases in para-equilibrium with the Compound Energy Formalism (CEF) within the CALPHAD method. This Python code has been integrated into a semi-automatic workflow to evaluate multicomponent phases. The code and workflow on the (Ce,La)Ni_5–H system have been validated with a data set from literature and own experiments. In this way, the ideal sorption properties of the (Ce,La)Ni_5–H system have been modeled thermodynamically with minimal user interference, and therefore also, the user-bias in the resulting thermodynamic data is reduced. The assessed sorption data includes the temperature-dependent plateau pressures and the hydrogen capacities as a function of hydrogen pressure.

The resulting thermodynamic data from the proposed approach has been discussed and led to new insights into the thermodynamic behavior of the system.

With the newly designed workflow, the active user time for a thermodynamic assessment is drastically reduced at the expense of computational time. As computational power increases with time and therefore computational methods in material science become increasingly important, this is intended as a first step towards a multidisciplinary predictive modeling approach for metal hydrides and the creation of a comprehensive thermodynamic database for metal hydrides of different material classes. Incorporating ab initio calculations enables the substitution of experimentally unavailable data to describe new alloying compositions or identify unknown material systems. This approach will significantly reduce the experimental time required to design and optimize metal hydrides for hydrogen technologies.

CRediT authorship contribution statement

Peter Hannappel: Writing – review & editing, Writing – original draft, Visualization, Software, Methodology, Investigation, Formal analysis, Data curation, Conceptualization. **Felix Heubner:** Writing – review & editing, Supervision, Conceptualization. **Mateusz Balcerzak:** Writing – review & editing, Visualization, Data curation. **Thomas Weißgärber:** Resources, Project administration, Funding acquisition.

Declaration of competing interest

The authors declare that they have no known competing financial interests or personal relationships that could have appeared to influence the work reported in this paper.

Acknowledgments

Project HYPHAD was selected in the Joint Transnational Call 2023 of M-ERA.NET 3, which is an EU-funded network of about 49 funding organisations (Horizon 2020 grant agreement No 958174). The project is funded by the Korea Institute for Advancement of Technology, South Korea, the National Science Centre, Poland, and the Sächsisches Staatsministerium für Wissenschaft, Kultur und Tourismus, Germany.

This research was financially supported by the Ministry of Trade, Industry and Energy (MOTIE) and Korea Institute for Advancement of Technology (KIAT) through the International Cooperative R&D program No. P0027799. This research was partially funded by the National Science Centre, Poland, number: 2023/05/Y/ST3/00249 under the M-ERA.NET 3 Call 2023. This project is co-financed with tax revenue on the basis of the budget adopted by the Saxon State Parliament.

Appendix A. Supplementary data

Supplementary material related to this article can be found online at https://doi.org/10.1016/j.actamat.2024.120529.

Data availability

The Electronic Supplementary Information attached to this article contains the raw and processed data necessary to reproduce the findings.

References

[1] M. Lototskyy, V. Yartys, B. Pollet, R. Bowman, Metal hydride hydrogen compressors: A review, Int. J. Hydrog. Energy 39 (11) (2014) 5818–5851, http://dx.doi.org/10.1016/j.ijhydene.2014.01.158.

[2] B. Chandrakala, K. Sarath Babu, E. Anil Kumar, Thermodynamic analysis of La and Mm based metal hydride pairs for solar energy-driven cold storage applications, Therm. Sci. Eng. Prog. 50 (2024) 102548, http://dx.doi.org/10.1016/j.tsep.2024.102548.

[3] B. Sakintuna, F. Lamari-Darkrim, M. Hirscher, Metal hydride materials for solid hydrogen storage: A review, Int. J. Hydrog. Energy 32 (9) (2007) 1121–1140, http://dx.doi.org/10.1016/j.ijhydene.2006.11.022.

[4] M. Witman, G. Ek, S. Ling, J. Chames, S. Agarwal, J. Wong, M.D. Allendorf, M. Sahlberg, V. Stavila, Data-driven discovery and synthesis of high entropy alloy hydrides with targeted thermodynamic stability, Chem. Mater. 33 (11) (2021) 4067–4076, http://dx.doi.org/10.1021/acs.chemmater.1c00647.

[5] S. Nations, T. Nandi, A. Ramazani, S. Wang, Y. Duan, Metal hydride composition-derived parameters as machine learning features for material design and H_2 storage, J. Energy Storage 70 (2023) 107980, http://dx.doi.org/10.1016/j.est.2023.107980.

[6] A. Rahnama, G. Zepon, S. Sridhar, Machine learning based prediction of metal hydrides for hydrogen storage, part I: Prediction of hydrogen weight percent, Int. J. Hydrog. Energy 44 (14) (2019) 7337–7344, http://dx.doi.org/10.1016/j.ijhydene.2019.01.261.

[7] H.L. Lukas, S.G. Fries, B. Sundman, Computational Thermodynamics: The Calphad Method, Cambridge University Press, 2007, pp. 1–313, http://dx.doi.org/10.1017/CBO9780511804137.

[8] M. Hillert, The compound energy formalism, J. Alloys Compd. 320 (2) (2001) 161–176, Materials Constitution and Thermochemistry. Examples of Methods, Measurements and Applications. In Memoriam Alan Prince, https://doi.org/10.1016/S0925-8388(00)01481-X.

[9] J.-M. Joubert, A Calphad-type equation of state for hydrogen gas and its application to the assessment of Rh–H system, Int. J. Hydrog. Energy 35 (5) (2010) 2104–2111, http://dx.doi.org/10.1016/j.ijhydene.2010.01.006.

[10] M. Palumbo, J. Urgnani, D. Baldissin, L. Battezzati, M. Baricco, Thermodynamic assessment of the H–La–Ni system, CALPHAD 33 (1) (2009) 162–169, http://dx.doi.org/10.1016/j.calphad.2008.09.003.

[11] E. Alvares, P. Jerabek, Y. Shang, A. Santhosh, C. Pistidda, T.W. Heo, B. Sundman, M. Dornheim, Modeling the thermodynamics of the FeTi hydrogenation under para-equilibrium: An ab-initio and experimental study, CALPHAD 77 (2022) 102426, http://dx.doi.org/10.1016/j.calphad.2022.102426.

[12] E.R. Pinatel, M. Palumbo, F. Massimino, P. Rizzi, M. Baricco, Hydrogen sorption in the $LaNi_{5-x}Al_x$-H system ($0 \leqslant x \leqslant 1$), Intermetallics 62 (2015) 7–16, http://dx.doi.org/10.1016/j.intermet.2015.03.002.

[13] P. Hannappel, E. Alvares, F. Heubner, C. Pistidda, P. Jerabek, T. Weißgärber, Thermodynamic assessment of the Ce-H and $CeNi_5$-H system, CALPHAD 85 (2024) 102701, http://dx.doi.org/10.1016/j.calphad.2024.102701.

[14] G. Zepon, B.H. Silva, C. Zlotea, W.J. Botta, Y. Champion, Thermodynamic modelling of hydrogen-multicomponent alloy systems: Calculating pressure-composition-temperature diagrams, Acta Mater. 215 (2021) 117070, http://dx.doi.org/10.1016/j.actamat.2021.117070.

[15] W. Oates, T.B. Flanagan, On the origin of increasing hydrogen pressures in the two solid phase regions of intermetallic compound-hydrogen systems, Scr. Metall. 17 (8) (1983) 983–986, http://dx.doi.org/10.1016/0036-9748(83)90435-0.

[16] P. Virtanen, R. Gommers, T.E. Oliphant, M. Haberland, T. Reddy, D. Cournapeau, E. Burovski, P. Peterson, W. Weckesser, J. Bright, S.J. van der Walt, M. Brett, J. Wilson, K.J. Millman, N. Mayorov, A.R.J. Nelson, E. Jones, R. Kern, E. Larson, C.J. Carey, İ. Polat, Y. Feng, E.W. Moore, J. VanderPlas, D. Laxalde, J. Perktold, R. Cimrman, I. Henriksen, E.A. Quintero, C.R. Harris, A.M. Archibald, A.H. Ribeiro, F. Pedregosa, P. van Mulbregt, SciPy 1.0 Contributors, SciPy 1.0: Fundamental algorithms for scientific computing in python, Nature Methods 17 (2020) 261–272, http://dx.doi.org/10.1038/s41592-019-0686-2.

[17] A. Al Alam, S. Matar, M. Nakhl, N. Ouaïni, Investigation of changes in crystal and electronic structures by hydrogen within $LaNi_5$ from first-principles, Solid State Sci. 11 (6) (2009) 1098–1106, http://dx.doi.org/10.1016/j.solidstatesciences.2009.02.026.

[18] J.F. Herbst, J. Hector, Hydrogen site energetics in $LaNi_5H_n$ and $LaCo_5H_n$: Toward predicting hydrides, Appl. Phys. Lett. 85 (16) (2004) 3465–3467, http://dx.doi.org/10.1063/1.1808503.

[19] T.B. Flanagan, W. Luo, J. Clewley, Calorimetric enthalpies of absorption and desorption of protium and deuterium by palladium, J. Less Common Metals 172–174 (1991) 42–55, http://dx.doi.org/10.1016/0022-5088(91)90431-3.

[20] H. Senoh, N. Takeichi, H.T. Takeshita, H. Tanaka, T. Kiyobayashi, N. Kuriyama, Hydrogenation properties of RNi_5 (R: rare earth) intermetallic compounds with multi pressure plateaux, Mater. Trans. 44 (9) (2003) 1663–1666, http://dx.doi.org/10.2320/matertrans.44.1663.

[21] S. Luo, J. Clewley, T.B. Flanagan, R. Bowman, L. Wade, Further studies of the isotherms of $LaNi_{5-x}Sn_x$–H for x=0–0.5, J. Alloys Compd. 267 (1) (1998) 171–181, http://dx.doi.org/10.1016/S0925-8388(97)00536-7.

[22] J.F. Lakner, T.S. Chow, Hydrides of $CeNi_5$, $MmNi_5$, $Ca_{0.2}(Ce_{0.65}Mm_{0.35})_{0.8}Ni_5$, $Ca_{0.2}Ce_{0.8}Ni_5$, $Ca_{0.2}Mm_{0.8}Ni_5$, and Mixed $CeNi_5$/$MmNi_5$, Report, University of North Texas Libraries, UNT Digital Library, 1982, URL https://digital.library.unt.edu/ark:/67531/metadc1212316/. [Accessed 5 January 2024].

[23] S. Klyamkin, V. Verbetsky, A. Karih, Thermodynamic particularities of some $CeNi_5$-based metal hydride systems with high dissociation pressure, J. Alloys Compd. 231 (1) (1995) 479–482, http://dx.doi.org/10.1016/0925-8388(95)01869-7.

[24] P. Zhou, J. Zhang, J. Bi, X. Xiao, Z. Cao, L. Zhan, H. Shen, M. Lu, Z. Li, Y. Zhao, L. Wang, M. Yan, L. Chen, Underlying factors of mega pressure hysteresis in cerium-rich $CaCu_5$-type metal hydrides and effective modification strategies, J. Mater. Chem. A 11 (2023) 25963–25972, http://dx.doi.org/10.1039/D3TA06351H.

[25] M. Odysseos, P. De Rango, C. Christodoulou, E. Hlil, T. Steriotis, G. Karagiorgis, G. Charalambopoulou, T. Papapanagiotou, A. Ampoumogli, V. Psycharis, E. Koultoukis, D. Fruchart, A. Stubos, The effect of compositional changes on the structural and hydrogen storage properties of (La–Ce)Ni_5 type intermetallics towards compounds suitable for metal hydride hydrogen compression, J. Alloys Compd. 580 (2013) S268–S270, SI : MH2012 https://doi.org/10.1016/j.jallcom.2013.01.057.

[26] A.A. Coelho, *TOPAS* and *TOPAS-Academic*: an optimization program integrating computer algebra and crystallographic objects written in C++, J. Appl. Crystallogr. 51 (1) (2018) 210–218, http://dx.doi.org/10.1107/S1600576718000183.

[27] H. Ye, M. Rong, Q. Yao, Q. Chen, J. Wang, G. Rao, H. Zhou, Phase equilibria and thermodynamic properties in the RE-Ni (RE = rare earth metals) binary systems, J. Mater. Sci. 58 (3) (2023) 1260–1292, http://dx.doi.org/10.1007/s10853-022-08039-1.

[28] H. Diaz, A. Percheron-Guégan, J. Achard, C. Chatillon, J. Mathieu, Thermodynamic and structural properties of $LaNi_{5-y}Al_y$ compounds and their related hydrides, Int. J. Hydrog. Energy 4 (5) (1979) 445–454, http://dx.doi.org/10.1016/0360-3199(79)90104-6.

[29] T. Kodama, The thermodynamic parameters for the $LaNi_{5-x}Al_x$–H_2 and $MmNi_{5-x}Al_x$–H_2 systems, J. Alloys Compd. 289 (1) (1999) 207–212, http://dx.doi.org/10.1016/S0925-8388(99)00173-5.